Electronic Supplementary Material (ESI) for Inorganic Chemistry Frontiers.

Supporting Information

Homochiral Cu_6Dy_3 single-molecule magnets displaying proton conduction and strong magneto-optical Faraday effect

Cai-Ming Liu,[1*] Shui-Dong Zhu,[2] Ying-Bing Lu,[2] Xiang Hao,[2] He-Rui Wen[3]

[1]*Beijing National Laboratory for Molecular Sciences, CAS Key Laboratory for Organic Solids, Institute of Chemistry, Chinese Academy of Sciences, Beijing 100190, China*
[2]*Jiangxi Key Laboratory of Function of Materials Chemistry, College of Chemistry and Chemical Engineering, Gannan Normal University, Ganzhou 341000, Jiangxi Province, China*
[3]*School of Metallurgy and Chemical Engineering, Jiangxi University of Science and Technology, Ganzhou 341000, Jiangxi Province, China*

Table of Contents

Table S1. Selected bond lengths (Å) and angles (°) of *R*-**1** and *S*-**1**.

R-**1**			
Dy1-O1W	2.350(5)	Dy1-O2	2.380(5)
Dy1-O2W	2.355(5)	Dy1-O6	2.362(5)
Dy1-O11	2.404(4)	Dy1-O12	2.366(4)
Dy1-O13	2.376(5)	Dy1-O14	2.408(5)
Dy2-O3W	2.361(5)	Dy2-O4W	2.353(5)
Dy2-O8	2.348(5)	Dy2-O10	2.372(5)
Dy2-O13	2.386(5)	Dy2-O14	2.387(5)
Dy2-O15	2.381(5)	Dy2-O16	2.395(4)
Dy3-O4	2.341(5)	Dy3-O5W	2.347(5)
Dy3-O6W	2.372(5)	Dy3-O11	2.378(5)
Dy3-O12	2.411(4)	Dy3-O15	2.414(5)
Dy3-O16	2.367(5)	Dy3-O30	2.365(5)
Cu1-O1	1.898(5)	Cu1-O2	1.942(5)
Cu1-O11	1.934(5)	Cu1-N1	1.904(6)
Cu2-O3	1.892(5)	Cu2-O4	1.956(5)
Cu2-O12	1.950(5)	Cu2N2	1.914(6)
Cu3-O7	1.896(5)	Cu3-O8	1.936(5)
Cu3-O13	1.956(5)	Cu3-N3	1.907(6)
Cu4-O5	1.903(5)	Cu4-O6	1.944(5)
Cu4-O14	1.953(4)	Cu4-N4	1.926(6)
Cu5-O15	1.948(5)	Cu5-O29	1.900(5)
Cu5-O30	1.958(5)	Cu5-N5	1.911(6)
Cu6-O9	1.901(5)	Cu6-O10	1.950(5)
Cu6-O16	1.942(5)	Cu6-N6	1.912(6)
O1-Cu1-O2	172.8(2)	N1-Cu1-O11	172.9(2)
O3-Cu2-O4	178.3(2)	N2-Cu2-O12	169.3(2)
O7-Cu3-O8	178.8(2)	N3-Cu3-O13	167.5(3)
O5-Cu4-O6	177.4(2)	N4-Cu4-O14	169.1(2)
O29-Cu5-O30	176.9(2)	N5-Cu5-O15	168.4(2)
O9-Cu6-O10	171.1(2)	N6-Cu6-O16	173.0(2)
S-**1**			
Dy1-O1W	2.352(4)	Dy1-O2	2.377(4)
Dy1-O2W	2.366(4)	Dy1-O6	2.354(4)
Dy1-O11	2.398(4)	Dy1-O12	2.380(4)
Dy1-O13	2.380(4)	Dy1-O14	2.414(4)
Dy2-O3W	2.362(5)	Dy2-O4W	2.358(5)
Dy2-O8	2.350(4)	Dy2-O10	2.370(4)
Dy2-O13	2.402(4)	Dy2-O14	2.390(4)
Dy2-O15	2.384(4)	Dy2-O16	2.401(4)
Dy3-O4	2.347(4)	Dy3-O5W	2.360(4)
Dy3-O6W	2.379(4)	Dy3-O11	2.371(4)

Dy3-O12	2.418(4)	Dy3-O15	2.415(4)
Dy3-O16	2.368(4)	Dy3-O30	2.363(4)
Cu1-O1	1.898(5)	Cu1-O2	1.951(4)
Cu1-O11	1.946(4)	Cu1-N1	1.909(5)
Cu2-O3	1.898(4)	Cu2-O4	1.964(4)
Cu2-O12	1.953(4)	Cu2-N2	1.923(5)
Cu3-O7	1.906(5)	Cu3-O8	1.957(5)
Cu3-O13	1.956(4)	Cu3-N3	1.917(5)
Cu4-O5	1.901(5)	Cu4-O6	1.950(5)
Cu4-O14	1.953(4)	Cu4-N4	1.923(5)
Cu5-O15	1.951(4)	Cu5-O29	1.906(5)
Cu5-O30	1.962(4)	Cu5-N5	1.905(5)
Cu6-O9	1.903(4)	Cu6-O10	1.956(4)
Cu6-O16	1.949(4)	Cu6-N6	1.918(5)
O1-Cu1-O2	172.6(2)	N1-Cu1-O11	173.4(2)
O3-Cu2-O4	178.4(2)	N2-Cu2-O12	170.1(2)
O7-Cu3-O8	179.5(2)	N3-Cu3-O13	168.1(2)
O5-Cu4-O6	177.1(2)	N4-Cu4-O14	169.0(2)
O29-Cu5-O30	176.7(2)	N5-Cu5-O15	168.1(2)
O9-Cu6-O10	171.4(2)	N6-Cu6-O16	172.8(2)

Table S2. Continuous Shape Measures calculation for the Dy1 atom in *R*-**1**.
Dy structures

OP-8	1 D8h	Octagon
HPY-8	2 C7v	Heptagonal pyramid
HBPY-8	3 D6h	Hexagonal bipyramid
CU-8	4 Oh	Cube
SAPR-8	5 D4d	Square antiprism
TDD-8	6 D2d	Triangular dodecahedron
JGBF-8	7 D2d	Johnson gyrobifastigium J26
JETBPY-8	8 D3h	Johnson elongated triangular bipyramid J14
JBTPR-8	9 C2v	Biaugmented trigonal prism J50
BTPR-8	10 C2v	Biaugmented trigonal prism
JSD-8	11 D2d	Snub diphenoid J84
TT-8	12 Td	Triakis tetrahedron
ETBPY-8	13 D3h	Elongated trigonal bipyramid

Structure[ML8]	OP-8	HPY-8	HBPY-8	CU-8	SAPR-8	TDD-8	JGBF-8	JETBPY-8	JBTPR-8	BTPR-8	JSD-8	TT-8	ETBPY-8
ABOXIY	28.334	22.496	14.451	8.199	**0.890**	1.459	15.207	28.148	2.798	2.266	4.544	8.855	23.459

Table S3. Continuous Shape Measures calculation for the Dy2 atom in *R*-**1**.
Dy structures

OP-8	1 D8h	Octagon
HPY-8	2 C7v	Heptagonal pyramid
HBPY-8	3 D6h	Hexagonal bipyramid
CU-8	4 Oh	Cube
SAPR-8	5 D4d	Square antiprism
TDD-8	6 D2d	Triangular dodecahedron
JGBF-8	7 D2d	Johnson gyrobifastigium J26
JETBPY-8	8 D3h	Johnson elongated triangular bipyramid J14
JBTPR-8	9 C2v	Biaugmented trigonal prism J50
BTPR-8	10 C2v	Biaugmented trigonal prism
JSD-8	11 D2d	Snub diphenoid J84
TT-8	12 Td	Triakis tetrahedron
ETBPY-8	13 D3h	Elongated trigonal bipyramid

Structure[ML8]	OP-8	HPY-8	HBPY-8	CU-8	SAPR-8	TDD-8	JGBF-8	JETBPY-8	JBTPR-8	BTPR-8	JSD-8	TT-8	ETBPY-8
ABOXIY	27.763	22.587	15.183	8.774	**0.672**	1.675	15.663	27.789	2.844	2.045	4.596	9.464	23.494

Table S4. Continuous Shape Measures calculation for the Dy3 atom in *R*-**1**.
Dy structures

OP-8	1 D8h	Octagon
HPY-8	2 C7v	Heptagonal pyramid
HBPY-8	3 D6h	Hexagonal bipyramid
CU-8	4 Oh	Cube
SAPR-8	5 D4d	Square antiprism
TDD-8	6 D2d	Triangular dodecahedron
JGBF-8	7 D2d	Johnson gyrobifastigium J26
JETBPY-8	8 D3h	Johnson elongated triangular bipyramid J14
JBTPR-8	9 C2v	Biaugmented trigonal prism J50
BTPR-8	10 C2v	Biaugmented trigonal prism
JSD-8	11 D2d	Snub diphenoid J84
TT-8	12 Td	Triakis tetrahedron
ETBPY-8	13 D3h	Elongated trigonal bipyramid

Structure[ML8]	OP-8	HPY-8	HBPY-8	CU-8	SAPR-8	TDD-8	JGBF-8	JETBPY-8	JBTPR-8	BTPR-8	JSD-8	TT-8	ETBPY-8
ABOXIY	27.730	22.771	15.366	8.842	**0.606**	1.931	15.757	27.768	2.916	2.030	5.041	9.472	23.718

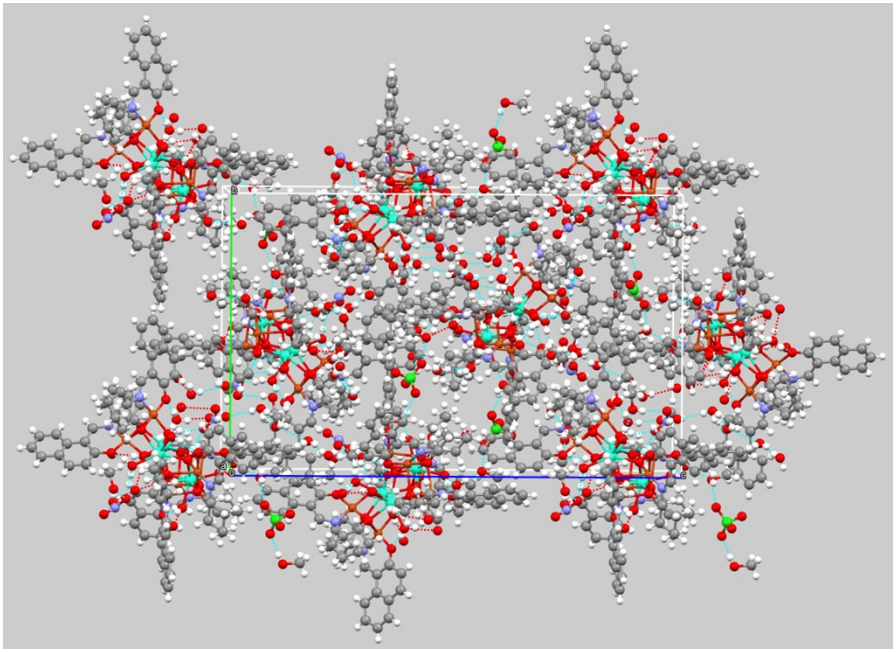

Fig. S1. Unit cell diagram of *R*-**1**.

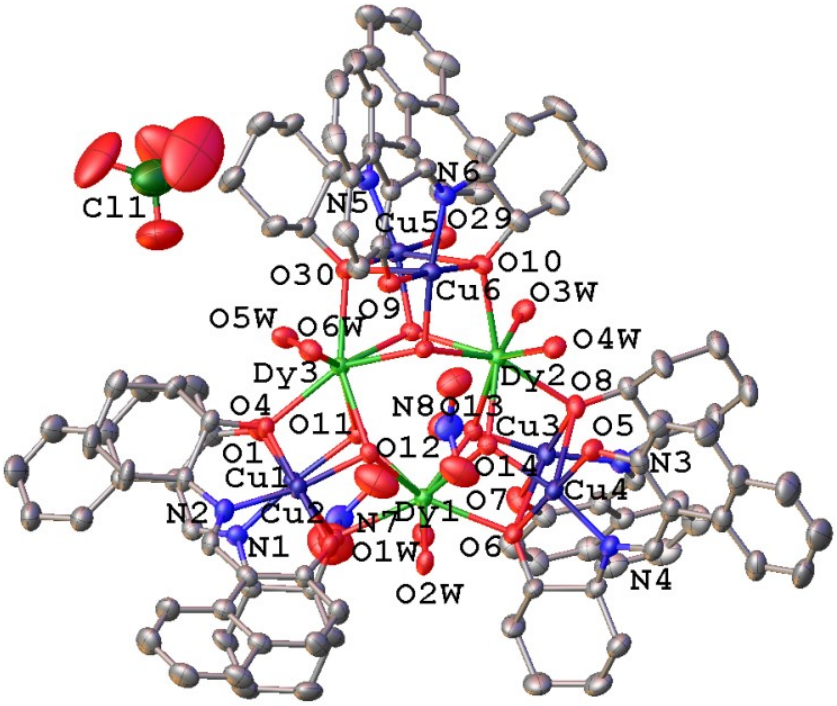

Fig. S2. Crystal structure of *S*-**1**, all H atoms and solvent molecules are omitted for clarity.

Table S5. Continuous Shape Measures calculation for the Dy1 atom in *S*-**1**.
Dy structures

OP-8	1 D8h	Octagon
HPY-8	2 C7v	Heptagonal pyramid
HBPY-8	3 D6h	Hexagonal bipyramid
CU-8	4 Oh	Cube
SAPR-8	5 D4d	Square antiprism
TDD-8	6 D2d	Triangular dodecahedron
JGBF-8	7 D2d	Johnson gyrobifastigium J26
JETBPY-8	8 D3h	Johnson elongated triangular bipyramid J14
JBTPR-8	9 C2v	Biaugmented trigonal prism J50
BTPR-8	10 C2v	Biaugmented trigonal prism
JSD-8	11 D2d	Snub diphenoid J84
TT-8	12 Td	Triakis tetrahedron
ETBPY-8	13 D3h	Elongated trigonal bipyramid

Structure[ML8]	OP-8	HPY-8	HBPY-8	CU-8	SAPR-8	TDD-8	JGBF-8	JETBPY-8	JBTPR-8	BTPR-8	JSD-8	TT-8	ETBPY-8
ABOXIY	28.345	22.521	14.490	8.125	**0.859**	1.446	15.400	28.136	2.857	2.230	4.551	8.781	23.500

Table S6. Continuous Shape Measures calculation for the Dy2 atom in *S*-**1**.
Dy structures

OP-8	1 D8h	Octagon
HPY-8	2 C7v	Heptagonal pyramid
HBPY-8	3 D6h	Hexagonal bipyramid
CU-8	4 Oh	Cube
SAPR-8	5 D4d	Square antiprism
TDD-8	6 D2d	Triangular dodecahedron
JGBF-8	7 D2d	Johnson gyrobifastigium J26
JETBPY-8	8 D3h	Johnson elongated triangular bipyramid J14
JBTPR-8	9 C2v	Biaugmented trigonal prism J50
BTPR-8	10 C2v	Biaugmented trigonal prism
JSD-8	11 D2d	Snub diphenoid J84
TT-8	12 Td	Triakis tetrahedron
ETBPY-8	13 D3h	Elongated trigonal bipyramid

Structure[ML8]	OP-8	HPY-8	HBPY-8	CU-8	SAPR-8	TDD-8	JGBF-8	JETBPY-8	JBTPR-8	BTPR-8	JSD-8	TT-8	ETBPY-8
ABOXIY	28.004	22.479	15.007	8.592	**0.713**	1.610	15.593	27.935	2.863	2.093	4.613	9.249	23.524

Table S7. Continuous Shape Measures calculation for the Dy3 atom in *S*-**1**.
Dy structures

OP-8	1 D8h	Octagon
HPY-8	2 C7v	Heptagonal pyramid
HBPY-8	3 D6h	Hexagonal bipyramid
CU-8	4 Oh	Cube
SAPR-8	5 D4d	Square antiprism
TDD-8	6 D2d	Triangular dodecahedron
JGBF-8	7 D2d	Johnson gyrobifastigium J26
JETBPY-8	8 D3h	Johnson elongated triangular bipyramid J14
JBTPR-8	9 C2v	Biaugmented trigonal prism J50
BTPR-8	10 C2v	Biaugmented trigonal prism
JSD-8	11 D2d	Snub diphenoid J84
TT-8	12 Td	Triakis tetrahedron
ETBPY-8	13 D3h	Elongated trigonal bipyramid

Structure[ML8]	OP-8	HPY-8	HBPY-8	CU-8	SAPR-8	TDD-8	JGBF-8	JETBPY-8	JBTPR-8	BTPR-8	JSD-8	TT-8	ETBPY-8
ABOXIY	27.629	22.851	15.438	8.836	**0.569**	2.030	15.763	27.903	2.831	1.942	5.184	9.451	23.617

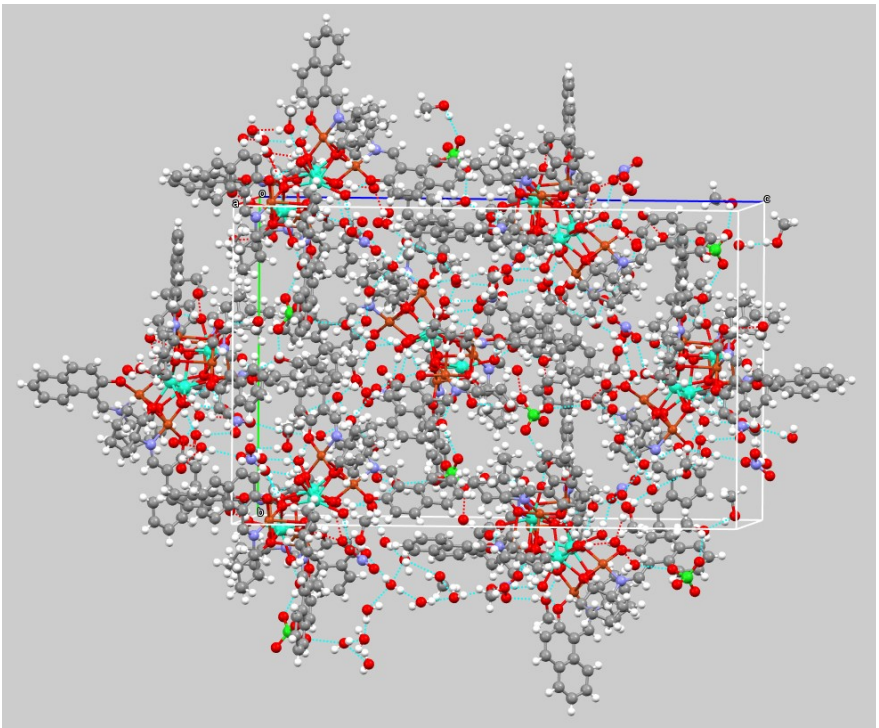

Fig. S3. Unit cell diagram of *S*-**1**.

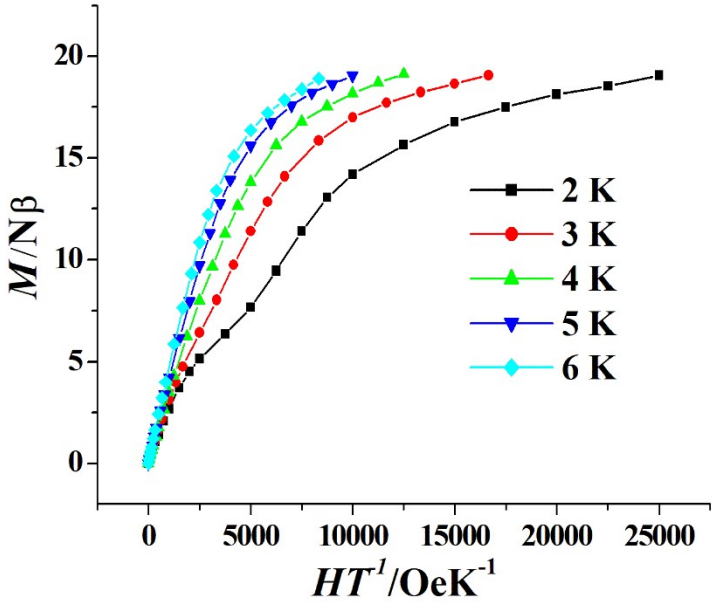

Fig. S4. *M versus H*/*T* plots at 2-6 K of *R*-**1**.

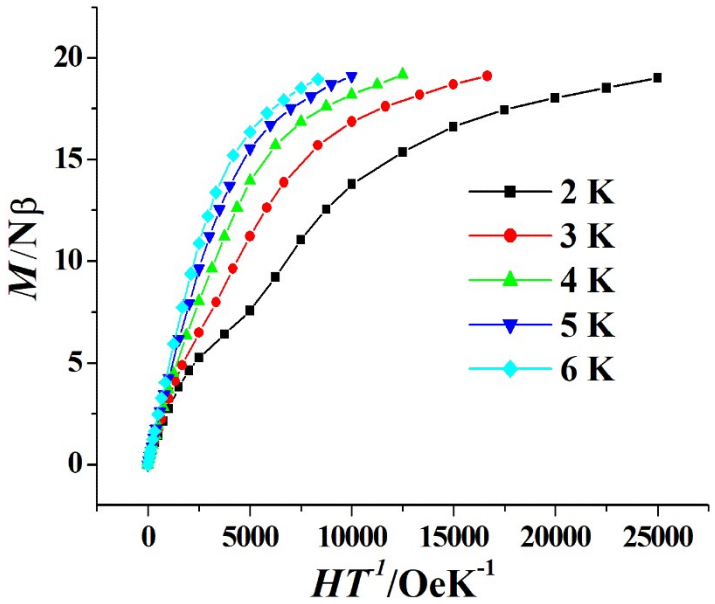

Fig. S5. *M versus H*/*T* plots at 2-6 K of *S*-**1**.

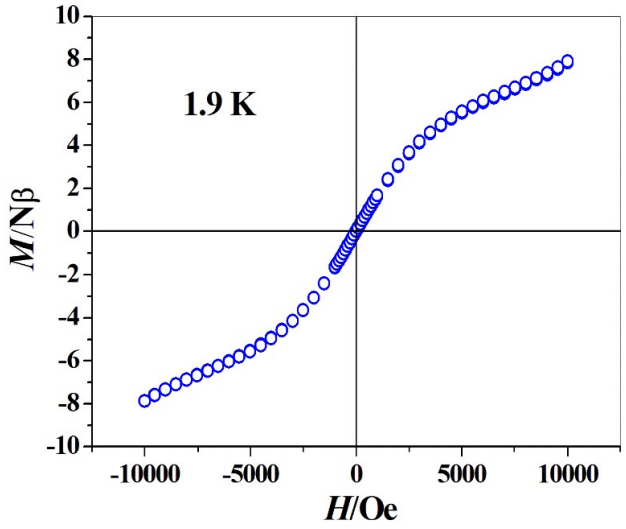

Fig. S6. Hysteresis loop for *R*-**1** at 1.9 K with the normal sweep rate (100-300 Oe min^{-1}).

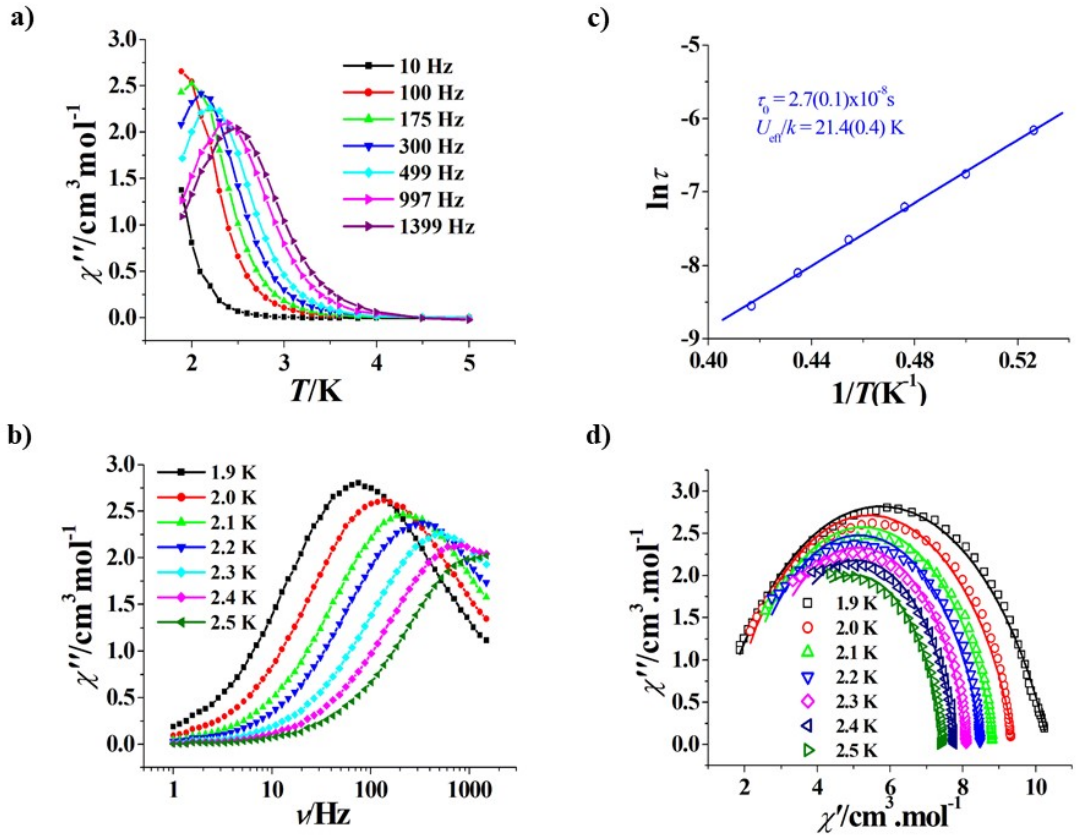

Fig. S7. Plots of χ'' *versus* T for *S*-**1** (H_{dc} = 0 Oe) (a). Frequency dependence of χ'' for *S*-**1** at zero dc field (b). Plot of $-\ln(\tau)$ *versus* $1/T$ for *S*-**1** (H_{dc} = 0 Oe), the solid line represents the best fitting with Arrhenius law (c). Cole-Cole plots measured from 1.9 to 2.5 K for *S*-**1** (H_{dc} = 0 Oe), the solid lines represent the best fitting with the generalized Debye model (d).

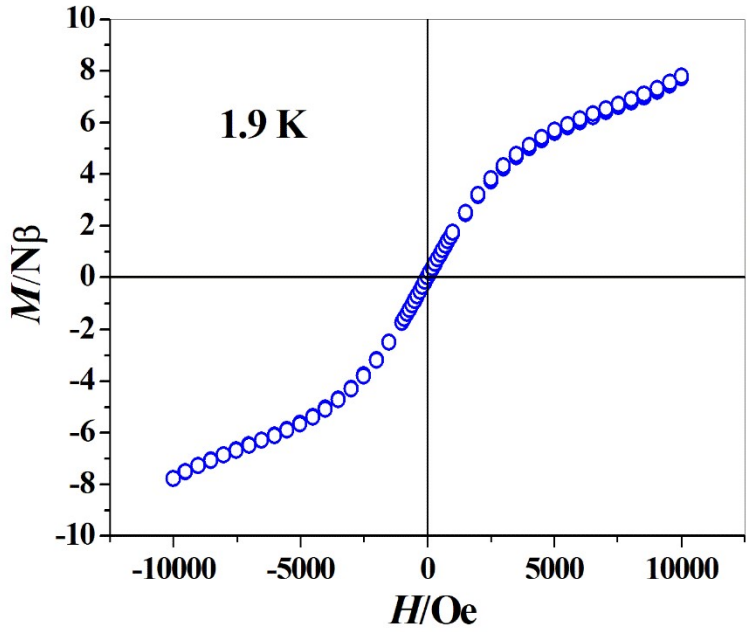

Fig. S8. Hysteresis loop for *S*-**1** at 1.9 K with the normal sweep rate (100-300 Oe min^{-1}).

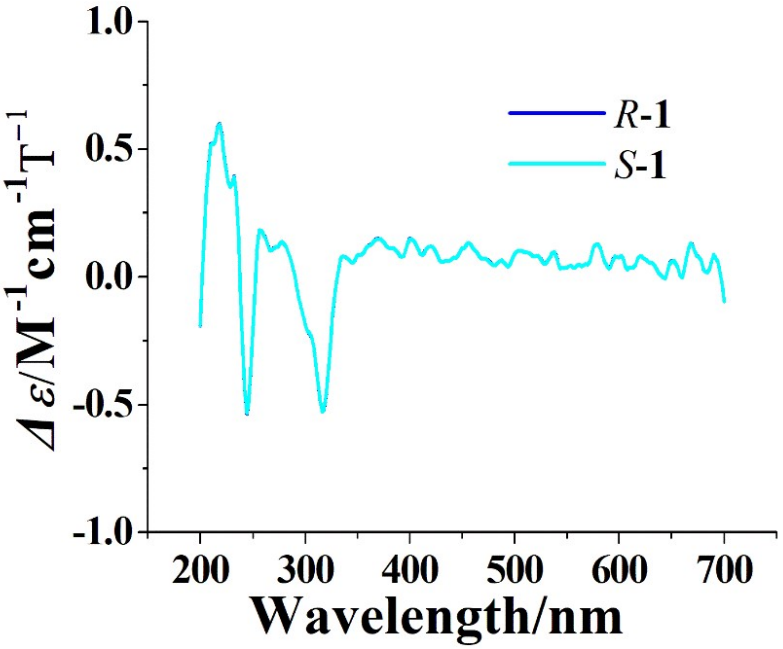

Fig. S9. MCD spectra of *R*-**1** and *S*-**1**.

Table S8. The proton conductivity of *R*-**1** at 25 °C under variable relative humidity (RH).

RH / %	σ / S cm^{-1}
60	6.85×10^{-8}
70	1.87×10^{-7}
80	3.97×10^{-7}
90	7.28×10^{-7}
100	9.55×10^{-7}

Table S9. The proton conductivity of *R*-**1** at 100 % relative humidity (RH) under variable temperature (°C).

Temperature / °C	σ / S cm^{-1}
25	9.55×10^{-7}
35	1.49×10^{-6}
45	1.99×10^{-6}
55	2.74×10^{-6}
65	3.34×10^{-6}
80	4.77×10^{-6}

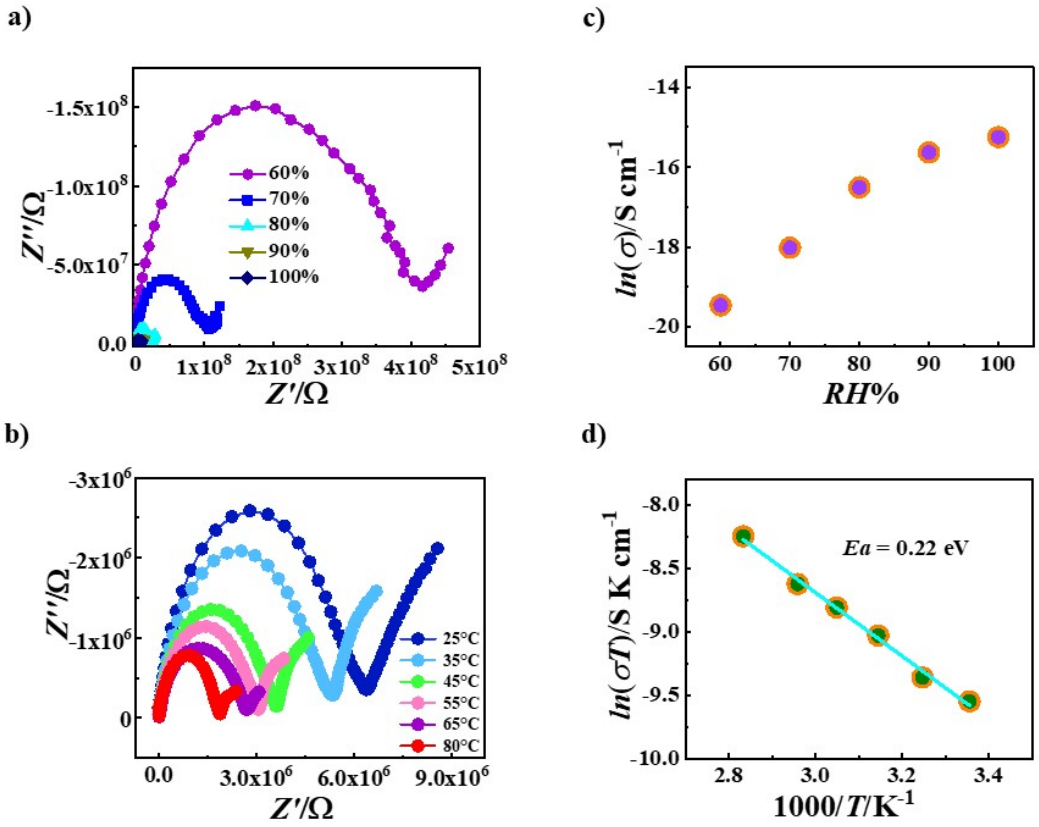

Fig. S10. Nyquist plots for *S*-**1** at 25 °C under different relative humidity (RH) levels (a). Nyquist plots for *S*-**1** at different temperatures under 100% relative humidity (RH) (b). Plots of proton conductivity for *S*-**1** *vs* RH at 25 °C (c). Plots of ln(σT) *vs* 1000/T for *S*-**1** under 100% relative humidity (RH) (d).

Table S10. The proton conductivity of *S*-**1** at 25 °C under variable relative humidity (RH).

RH / %	σ / S cm^{-1}
60	3.54×10^{-9}
70	1.49×10^{-8}
80	6.78×10^{-8}
90	1.62×10^{-7}
100	2.40×10^{-7}

Table S11. The proton conductivity of ***S*-1** at 100 % relative humidity (RH) under variable temperature (°C).

Temperature / °C	σ / S cm^{-1}
25	2.40×10^{-7}
35	2.78×10^{-7}
45	3.77×10^{-7}
55	4.57×10^{-7}
65	5.33×10^{-7}
80	7.45×10^{-7}